Phase Transitions
Publication details, including instructions for authors and subscription information:
http://www.informaworld.com/smpp/title~content=t713647403

Effect of alanine doping on the low-frequency Raman Modes in triglycine sulphate crystals at 12 K

P. K. Bajpai [a]; N. K. Chandan [a]; Hemraj Singh [a]; A. L. Verma [b]
[a] School of Pure and Applied Physics, Guru Ghasidas University, Bilaspur 495 009, India [b] Department of Physics, North-Eastern Hill University, Shillong 793 022

Online Publication Date: 01 November 2003

To cite this Article Bajpai, P. K., Chandan, N. K., Singh, Hemraj and Verma, A. L.(2003)'Effect of alanine doping on the low-frequency Raman Modes in triglycine sulphate crystals at 12 K',Phase Transitions,76:11,935 — 944
To link to this Article: DOI: 10.1080/0141159021000037448
URL: http://dx.doi.org/10.1080/0141159021000037448

Phase Transitions
Vol. 76, No. 11, November 2003, pp. 935–944

Taylor & Francis
Taylor & Francis Group

EFFECT OF ALANINE DOPING ON THE LOW-FREQUENCY RAMAN MODES IN TRIGLYCINE SULPHATE CRYSTALS AT 12 K

P.K. BAJPAI[a,*], N.K. CHANDAN[a], HEMRAJ SINGH[a] and A.L. VERMA[b]

[a]*School of Pure and Applied Physics, Guru Ghasidas University, Bilaspur 495 009, India;*
[b]*Department of Physics, North-Eastern Hill University, Shillong 793 022*

(Revised 30 April 2001; In final form 27 July 2002)

Low-temperature Raman spectra of pure, and alanine doped triglycine sulphate (TGS) crystals in the low-frequency range $\nu < 400\,cm^{-1}$ are reported. Substantial changes in the relative intensity of several modes occur whereas the band positions remain largely unchanged. Doping induced relative intensity changes are correlated with the change in H-bonding and molecular reorientation. Results indicate that alanine replaces G(I) mainly at low-dopant concentration. However, doping causes reorientation of all the three ions.

Keywords: Ferroelectrics; Dopants; Raman spectra of crystals; Lattice modes; Triglycine sulphate

INTRODUCTION

Triglycine sulphate (TGS) belongs to an important family of ferroelectric materials, suitable for pyroelectric detector applications (Lock, 1971). It undergoes a structural phase transition from paraelectric (PE) to ferroelectric (FE) phase at 322 K (Matthias *et al.*, 1956). The major problem associated with this crystal, when used as a pyroelectric detector element, is the polarization reversal with time. Modifications using inorganic, organic and iso-structural dopants, as well as defects induced by irradiation (Bye *et al.*, 1972; Bhalla *et al.*, 1983; Gaffar and Abu El-Fadl, 1988; Ravi *et al.*, 1994; Stankowska *et al.*, 1994; Kampysheva *et al.*, 1995; Aravazhi *et al.*, 1997; Bajpai *et al.*, 1999) were tried to overcome this problem. However, problems such as noise equivalent power (NEP), cracking, high Barkhausen noise, etc. arise with these modifications. Moreover, such modifications do not lead to optimum changes in all the relevant physical properties essential for better detector performance. Critical evaluation of the experimental results, reported in the literature on dopant induced changes in TGS, revealed that almost all attempts were mainly focused toward obtaining the desired changes in the values of various parameters. Studies using concentration of dopant as a parameter, to understand the nature of changes in the relevant physical properties, are scant. In fact, any improvement

*Corresponding author. E-mail: bajpai_pk©yahoo.com

ISSN 0141-1594 print: ISSN 1029-0338 online © 2003 Taylor & Francis Ltd
DOI: 10.1080/0141159021000037448

in detector performance requires that changes due to doping in terms of molecular dynamics of various subspecies of TGS should be known. We have, therefore, undertaken a vibrational study of these changes with dopant concentration. In our earlier paper (Santra *et al.*, 1994), the room temperature Raman spectra of alanine doped TGS were analyzed. We have also been able to identify some of the modes arising due to distinct glycine ions, viz. G(I), G(II) and G(III). Since at room temperature the modes were not resolved, we have studied the low-temperature (12 K) Raman spectra of these systems. It is expected that most of the lattice modes should be well resolved and sharp at low temperature. Low-frequency modes are also expected to reflect the change in the orientational dynamics of molecular units caused by doping.

A large number of vibrational studies on TGS are reported, including the low-temperature and low-frequency spectra (Barker and Tinkham 1963; Quilichini *et al.*, 1969; Koneko *et al.*, 1974; Cerevenka *et al.*, 1976; Schaack and Winterfeldt, 1977; Winterfeldt *et al.*, 1977; Huong and Hilczer 1981; Komyak *et al.*, 1993; Santra *et al.*, 1994; Malyarevich and Posledovich 1996). Quilichini *et al.* (1969) measured the temperature dependence of polarized Raman spectra below 200 cm^{-1}, but failed to see significant spectral changes due to the phase transition. Koneko *et al.* (1974) measured the temperature dependence of the lattice modes. They determined the symmetry species of the observed modes and could assign some of them. Cerevenka *et al.* (1976) reported the room temperature behaviour of the lattice vibrations in TGS using Raman spectra. The most systematic vibrational study on TGS was reported by Schaack and Winterfeldt (1977). They investigated the infrared and Raman spectra of TGS and TGSe at several temperatures, and supported the order–disorder mechanism of the transition, using information about the temperature dependent changes in line widths, frequencies, intensities and lifting of quasi degeneracy of certain modes. Most of the observed lines could be attributed to the motion of different molecular groups in the crystal. With regard to the vibrational study of doped systems, the reports are scant (Bhalla *et al.*, 1983; Santra *et al.*, 1994; Jin and Bhalla, 1995). The room temperature Raman studies by us have been carried out on crystals having alanine concentrations *in the solution* ranging from 0.5 mol% to 20 % at five different concentrations. The relative intensity ratio of some lattice modes in this study has shown a reversal of intensity with increase in dopant concentration. Low-temperature experiments were therefore performed to examine the similar behaviour with better-resolved modes. We concentrated on only three crystals, i.e. pure TGS and the two grown with minimum and maximum concentrations of alanine in the growth solution.

EXPERIMENTAL

Single crystals of pure as well as alanine doped TGS were grown from aqueous solution. Glycine, alanine and sulfuric acid were taken in appropriate quantities in solution. The concentrations of alanine reported in this work are the nominal concentrations used in the solution for crystal growth. The actual content of the alanine in the crystal differs from this. The dielectric data taken from the same set of crystals (Chandan and Bajpai, 2002) clearly show the reduction in the dielectric peak with increasing percentage of alanine in the growth solution. This implies that increasing amount of alanine is being incorporated in the crystal of TGS with increasing percentage of alanine in solution.

The grown crystals were in the form of thick plates with broad faces parallel to the *b*-axis. The crystals were cut in the form of rectangular parallelopipeds and the faces were polished. In some published reports, the *b*-axis is considered parallel to the *X*-direction, while in others it is taken as the *Y*- or *Z*-axis. In this work we have followed the configuration used by Koneko *et al.* (1974). Accordingly, the A-type vibrational species would be observable in the XX, YY, ZZ, XY scattering geometries and the B-type in YZ, ZX geometries. Polished crystals were afixed at the tip of the cryo-cooler under high vacuum. Temperature was maintained at 12 K with a stability of $\pm 1^{\circ}$C. All the Raman spectra were recorded on SPEX Ramalog 1403 double monochromator equipped with a cooled RCA-31034A photo multiplier tube and a photon counting system. The excitation source was 488-nm laser line from Ar^{+} laser (model Spectra Physics 165-09). The slit band pass was 2 cm^{-1} and the power at the sample was 100 mW.

ENUMERATION OF PHONONS

TGS belongs to the monoclinic system in both phases, with space groups $P2_1/C_2^2$ and $P2_1/m/C_{2h}^9$ below and above the phase transition, respectively (Hoshino *et al.*, 1959). The unit cell contains three crystallographically distinguishable glycine ions: the zwitterion $NH_3{}^{+}CH_2COO^{-}$ termed G(II) and the two glycinium ions $NH_3{}^{+}CH_2COOH$. One glycinium ion (G(I)) is in the form of a monomer, $(NH_3{}^{+}CH_2COOH)G_m^{1+}$ having weak hydrogen bonding with one of the oxygens of SO_4^{2-}, while the other glycinium ions (G(III)) forms a dimer with G(II) through a relatively stronger hydrogen bond. Thus the general formula is written as $G_d^{1+}G_m^{1+}SO_4^{2-}$ or $(NH_3{}^{+}CH_2COO^{-})$ $(NH_3{}^{+}CH_2COOH)_2$ SO_4^{2-}. There are two molecules in each unit cell, as shown in Fig. 1. Accordingly, there are 222 total number of motions. The four types of large molecular groups in each unit cell give rise to motions which correspond to low energy

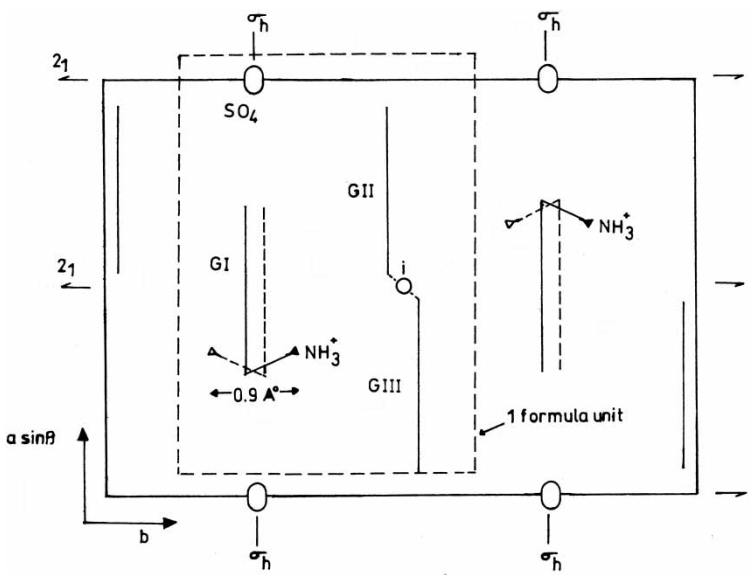

FIGURE 1 Schematic [001] projection of the elementary unit cell of TGS. G (I), G (II) and G (III) are three crystallographically distinct glycine ions in the FE phase.

TABLE I Classification of lattice vibrations of TGS in the ferroelectric phase

Space group	*Symmetry species*	*Translational modes*	*Librational modes**	*IR active*	*Raman active*
C_2^9–$P2_1$	A	11	12 (3)	μ_z	α_{xx} α_{yy} α_{zz} α_{xy}
	B	10	12 (3)	μ_x, μ_y	α_{yz} α_{xz}

*Numbers in parentheses denote the number of librational mode of SO_4^{2-}.

Raman modes or external phonons. There are 48 such phonons, out of which three represent the acoustic modes. Remaining 45 modes of motion are optic modes. These are associated with translational and librational motions of G(I), G(II), G(III) and SO_4^{2-} (lattice modes). Group theoretical analysis of the number of different symmetry species in the ferroelectric phase for external modes at $k = 0$ (center of Brillouin zone) is given in Table I. Accordingly, there are (11A + 10B) translational and (12A + 12B) librational modes. The A-type modes will appear in Y(XX)Z, X(YY)Z, X(ZZ)Y and Y(XY)Z polarization geometries, and the B-type in Y(XZ)X and X(YZ)Y geometries.

RESULTS AND DISCUSSION

Polarized Raman spectra in Y(XX)Z (A-type) and X(YZ)Y (B-type) polarization geometries are shown in Fig. 2. In Table II we summarize the relative peak intensity and normalized peak intensity of bands observed in A–B-type geometries. These bands could be attributed to the three types of mode of motions. Bands observed below 150 cm^{-1} are largely due to librational and translational motions of the three glycine ions and SO_4^{2-}, whereas bands above 300 cm^{-1} are due to torsional vibrations around C–C bonds. Bands observed in the in-between region have main contribution from lattice modes associated with hydrogen bonds and $So_4{}^{2-}$. Torsional vibrations around C–C bonds are assigned as 388 cm^{-1}–G(I); 342 cm^{-1}–G(III); and 328 cm^{-1}–G(II). Assignments of observed bands are made based on earlier reports, comparison with room temperature spectra, and lattice modes observed in glycine crystal. The band observed at 55 cm^{-1} in the PE phase splits into four components at low temperature. Components at 57 and 67 cm^{-1} are assigned to collective vibrations of SO_4^{2-} group, whereas those at 73 and 77 cm^{-1} are due to G_m^{1+} monomer, which is the result of weakening of ionic interaction between G_m^{1+} and SO_4^{2-}. The band at 36 cm^{-1} is assigned to G(I) translational mode, whereas bands at 70 and 100 cm^{-1} are associated with G(II) and G(III), respectively (Cerevenka *et al.*, 1976). The bands at 45, 137 and 170 cm^{-1} are associated with SO_4^{2-}. Bands around 200 cm^{-1} (21, 213 and 201 cm^{-1}) are associated with H-bond.

In order to investigate the effect of alanine doping in TGS, we have analyzed the band positions and relative intensities of lattice modes in the spectra of pure and doped crystal. The following observations are drawn from this

(i) The observed band positions remain almost invariant with doping except for bands at 231 and 270 cm^{-1} in YZ geometry, which shift at 226 and 254 cm^{-1} for 0.5% doped sample spectra, and revert back to the original position in 20% sample spectra.

(ii) The band observed at 124 cm^{-1} in YY geometry becomes asymmetric at 0.5% doping and splits into two bands at 124 and 118 cm^{-1} in 20% doping.

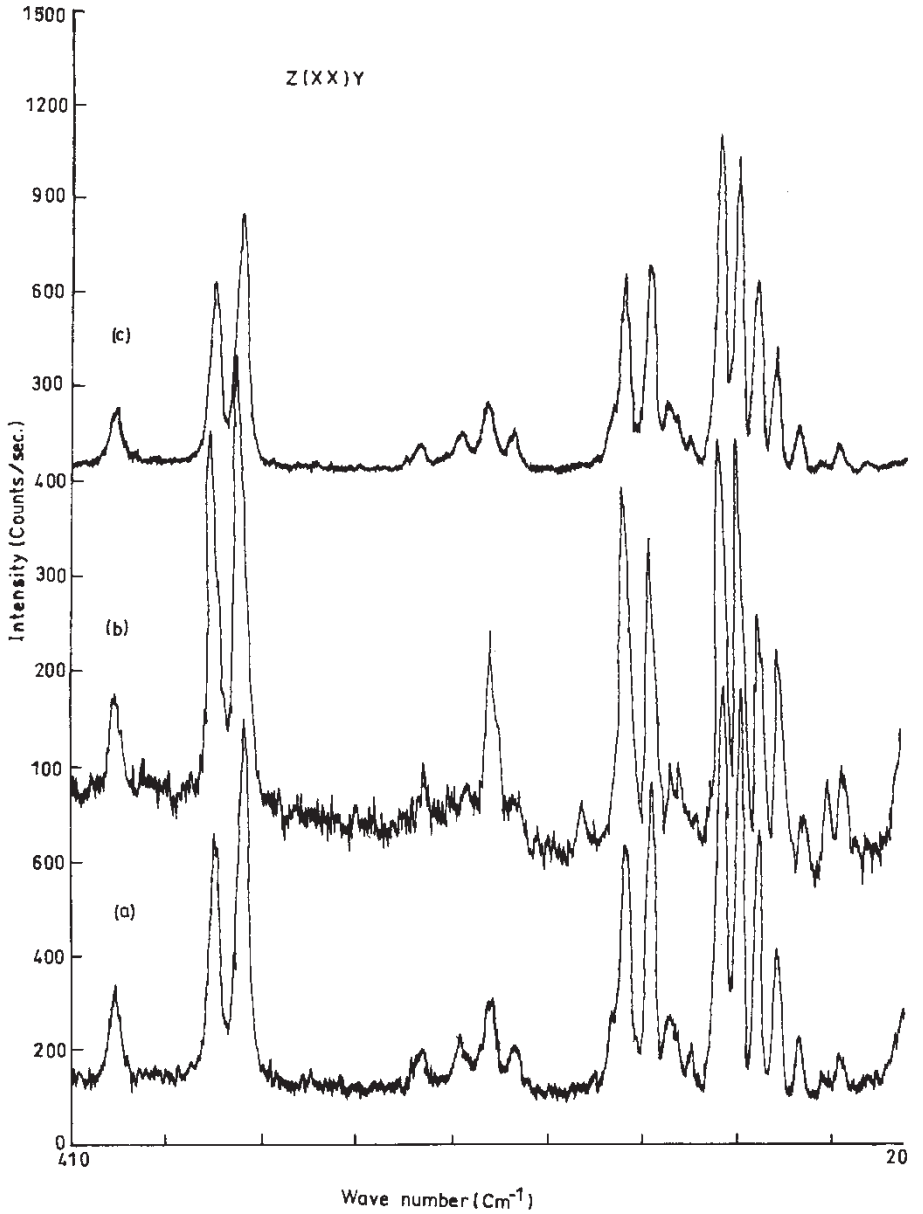

FIGURE 2a Observed low-frequency modes in Z(XX)Y scattering geometry: (a) pure TGS; (b) TGS grown with 0.5% alanine in solution; and (c) TGS grown with 20% alanine (A-phonons) in solution. Relative intensities of bands in different spectra have different scales. Numbers near–top of the peak are band positions in cm^{-1}.

Similar splitting is observed for the band at 244 cm^{-1}, which splits into two bands at 221 and 254 cm^{-1} with doping.

(iii) In XY polarization, the band at 141 cm^{-1} with shoulder at 147 and 157 cm^{-1} becomes single band at 141 cm^{-1} at 0.5% sample, and reappears as three band structure for 20% sample.

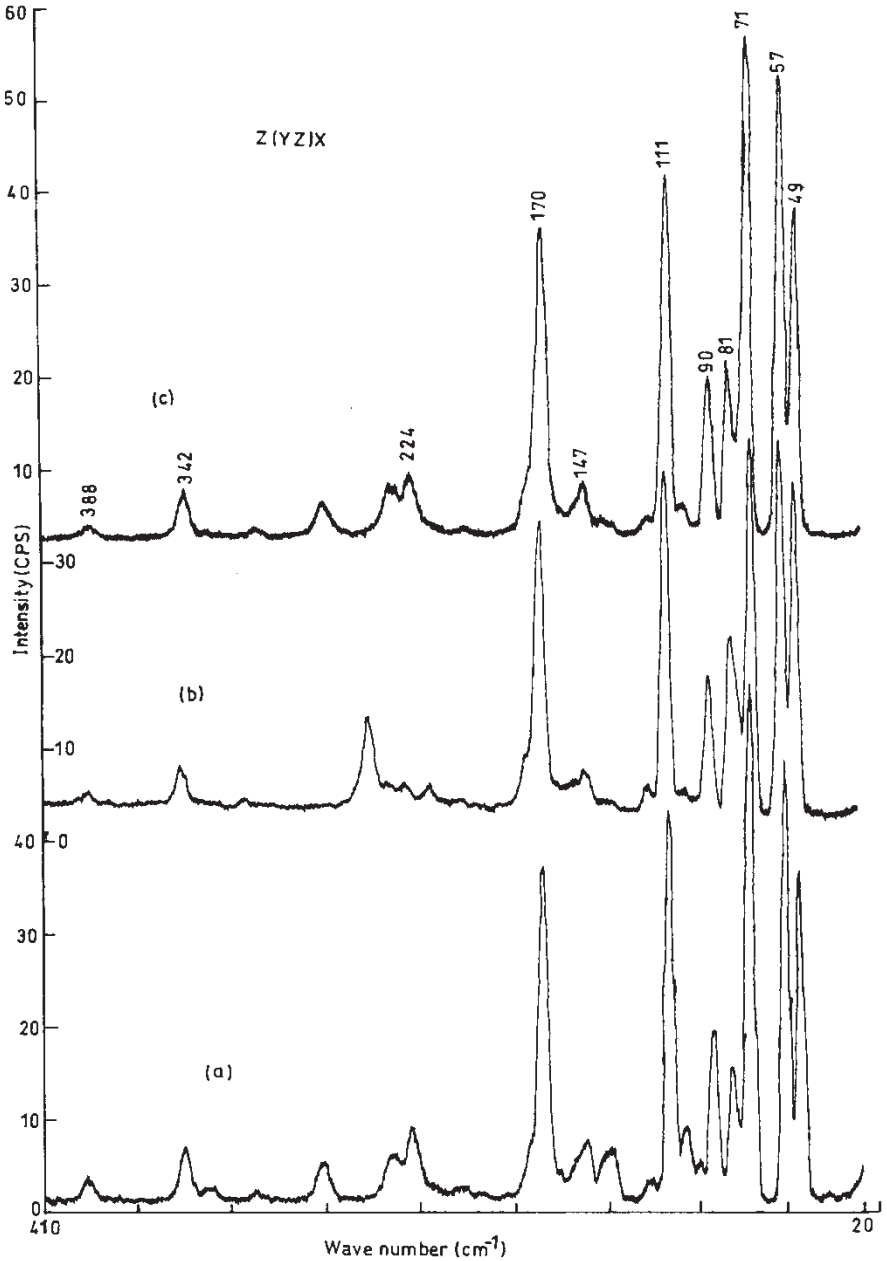

FIGURE 2b Observed low-frequency modes in X(YZ)Y scattering geometry: (a) pure TGS; (b) TGS grown with 0.5% alanine; and (c) TGS grown with 20% alanine (A-phonons). Relative intensities of bands in different spectra have different scales. Numbers near–top of the peak are band positions in cm^{-1}.

(iv) Relative intensities of several bands change in 0.5%-doped crystal and the intensity patterns revert almost to that of pure system in 20% doped crystal. The intensity changes are more pronounced in A-type modes than in B-type modes.

TABLE IIa Wave numbers, relative band intensity and normalized peak intensity of observed bands in X(YY)Z scattering geometry

Band position in cm^{-1}	*Relative intensity in counts per second*			*Normalized peak intensity in counts per second*			*Assignments*
	TGS pure	*TGS + 0.5% alanine*	*TGS + 20% alanine*	*TGS pure*	*TGS + 0.5% alanine*	*TGS + 20% alanine*	
388	440	523	908	4.6	7.6	7.0	Torsional vib. C–C G(I)
370	104		87				–
342	403	264	621	4.2	3.8	4.8	Torsional vib. C–C G(III)
330	321	229	404	3.4	3.3	3.1	Torsional vib. C–C G(II)
314		40	62	0.5	0.5	0.5	
300	323	50	93	0.6	0.7	0.7	
254		124	112	0.9	1.8	0.9	
241	313	269	485	3.3	3.9	3.7	
226	231	284	429	2.4	4.1	3.3	H-bond lattice
213		55	68				H-bond lattice
201	90	50	131	0.9	0.7	1.0	H-bond lattice
170	254	119	299	2.7	1.7	2.3	SO_4^{2-} libration
148	612	418	902	6.4	6.1	7.0	
137	1246	975	2201	13.0	14.1	17.0	SO_4^{2-} trans–libration
124	515	129	317	5.4	1.9	2.4	Gly/SO_4^{2-} trans–libration
111		378	727		5.5	5.6	
104	1418	915	2096	14.8	13.3	16.2	Glycine lib–trans G(I)
97	948	557	864	9.9	8.1	6.7	Glycine lib G(II)–G(III)
87	836	671	1001	8.7	9.7	7.7	
68	403	129	336	4.2	1.9	2.6	
57	418	164	230	4.4	2.4	1.8	SO_4^{2-} collective vibration
45	701	388	460	7.3	5.6	3.6	SO_4^{2-} libration
36	321	219	286	3.4	3.2	2.2	G(I) translation

TABLE IIb Wave numbers, relative band intensity and normalized peak intensity of observed bands in X(YZ)Y scattering geometry (B-phonons)

Band position in cm^{-1}	*Relative intensity in counts per second*			*Normalized peak intensity in counts per second*			*Assignments*
	TGS pure	*TGS + 0.5 % alanine*	*TGS + 20 % alanine*	*TGS pure*	*TGS + 0.5 % alanine*	*TGS + 20% alanine*	
389	149	105	87	1.0	0.7	0.6	Torsional vib. C–C G(I)
342	348	269	274	2.4	1.9	2.0	Torsional vib. C–C G(III)
276	224		200	1.5		1.4	
243	261	220	294	1.8	1.5	2.1	H-bond lattice
234	410	180	361	2.8	1.3	2.6	–
171	1816	1866	1667	12.5	12.9	11.9	SO_4^{2-} libration
147	335	284	311	2.3	2.0	2.2	
137	286	75	112	2.0	0.5	0.8	SO_4^{2-} translation–libration
120	100	179	112	0.7	1.2	0.8	
111	2101	2194	1953	14.4	15.2	14.0	
90	883	896	871	6.1	6.2	6.2	Glycine libration
81	721	1149	771	5.0	8.0	5.5	
71	2786	2433	2711	19.0	16.4	19.4	
57	2363	2418	2487	16.2	16.8	17.8	SO_4^{2-} collective vibration
49	1766	2149	1779	12.1	14.9	12.7	SO_4^{2-} libration

The apparent splitting of some bands as discussed above may not be due to change in site potential or dynamical splitting because the split components are observed as separate bands in other polarization geometries in pure crystal. Therefore, the major effect of alanine doping seems to be the reduction or enhancement of intensities of some bands.

In order to understand these intensity changes more clearly, we calculated the normalized peak intensity (%) of each band defined as

$$I_{\mathrm{NPI}} = (I_{\mathrm{peak}} / \sum I_{\mathrm{peak}})^{*}100 \tag{1}$$

Here the summation is taken over all observed bands up to $\nu = 400\,\mathrm{cm}^{-1}$ in a particular scattering geometry. Normalized peak intensities so calculated should indicate the reduction–enhancement in the intensities of the individual modes. It may be mentioned that NPI values are estimated from the observed peak intensities measured manually from the spectra, which has measurement error of 0.5 to 1% in calculated values. For weak band, this may not be reliable; a slight misalignment of polarization geometry will give rise to comparable intensities of leakage modes. In fact, the error level will be comparable to the estimated NPI in many weak features. We have therefore considered only those modes for discussion where NPI change is much beyond the error level. Typical NPI values estimated from the above procedure are given in Table II.

The fact that doping of alanine hardly changes the frequency of external modes points towards the site replacement of dopant. The observed relative intensities of low-frequency modes in different polarization geometries show systematic changes. In B-type geometries most of the observed bands do not change the doping. Even the bands which change show change in intensity for 20% doped samples, with the exception of three bands in YZ polarization (49.5, 71 and 81 cm^{-1}) which show reversal behaviour. This could be taken as evidence of doping inducing the derived polarizability component during mode motions primarily towards *b*-axis (*Z*-axis). The NPI changes are significant in bands at 87, 97, 104, 137 cm^{-1} in all A-type geometries; 213 cm^{-1} in XX and XY; 36, 45 and 170 cm^{-1} in YY and XY polarization geometry. In all A-type geometries same bands undergo intensity changes. The band at 36 cm^{-1}, assigned to G(I) translational mode (Koneko *et al.*, 1974), show intensity reduction–enhancement in YY–XY, respectively, with doping. This suggests that the translational motion of G(I) is affected by doping.

The bands at 45, 57, 137 and 170 cm^{-1} associated with SO_4^{2-} also show intensity changes; the nature of intensity change in the former two bands are correlated with that of 36 cm^{-1} band intensity change. The intensity change in these bands clearly indicates the involvement of G(I) as the SO_4^{2-} is interlinked with G(I) through H-bond. 213 and 221 cm^{-1} bands, associated with H-bonding, also show intensity changes; 213 cm^{-1} showing larger change in comparison to 221 cm^{-1} band. 213 cm^{-1} may, therefore, be due to SO_{4}- G_m^{1+}. The bands at 69, 97 and 104 cm^{-1} are attributed to librational motions of glycine ions. These modes undergo drastic intensity reversal reflecting the reorientational change being the major change due to doping. This suggests that glycine ions reorient with doping, changing the intensity distribution of modes in various polarization geometries. Further, the higher sensitivity of A-modes at low-doping concentration indicates that the derived polarizability during the motion is influenced by the dipolar interaction along *b*-axis. However, the redistribution of intensity and change

in B-type mode intensities in 20% alanine grown crystals reveal that high concentration of doping does not restrict the interaction along the polar axis. At 20% doping, further realignment of molecular ions take place and the spectrum approaches that of pure crystal. This essentially means that at higher concentration, dopant dipoles are not isolated and interact with other dipoles, thus reorienting all glycine molecules. Further, alanine prefers specific glycine ion site, as some of the modes are insensitive to doping.

The study of lattice vibrations thus indicates that modes showing changes with alanine doping are associated with either G(I) or SO_4^{2-}/H-bond between them. Further, the modes which show intensity change mainly at 20% alanine concentration (in B-type scattering geometries are associated with G(II) and G(III).

CONCLUSIONS

Low-temperature Raman spectral analysis of lattice modes in pure and alanine substituted TGS single crystals reveals that, in crystals grown even with rather high concentration of alanine in the growth solution, the dopant replaces the glycine substitutionally. The librational and translational modes of all three glycine ions in such alanine substituted TGS crystals show change in relative intensity. At low concentration of alanine doping, the intensity changes are mainly restricted to A-type modes. At higher concentration of alanine, both A–B-types modes show intensity changes. However, clear-cut conclusion about the site of replacement could not be inferred as the external modes are highly mixed modes. Probably, a better picture will emerge from the analysis of internal modes at low temperature.

Acknowledgement

Financial assistance received by PKB from the Department of Science and Technology, New Delhi (Grant No. SP/S2/M-55), is gratefully acknowledged.

References

Aravazhi, S., Jayavel, R. and Subramanian, C. (1997). Growth and characterization of ℓ-alanine and ℓ-valine doped tri-glycine sulphate crystals. *Material Research Bulletin*., **32**, 1503.

Bajpai, P.K., Chandan, N.K., Tiwari, H.S., Kundu, T. and Chakravorty, D. (1999). *Proceedings of DAE Solid State Physics Symposium*, **42**, 203.

Barker, A.S. and Tinkham, M. (1963). Far infra-red dielectric measurements on potassium di-hydrogen phosphate, tri-glycine sulphate, and rutile. J. *Chem. Phys*., **38,** 2257.

Bhalla, A.S., Fang, C.S., Yao, Xi and Cross, L.E. (1983). Effect of organic dopants on the pyroelectric properties of TGS. *Appl. Phys. Lett*., **43**, 932.

Bye, K.L., Whipps, P.W. and Keve, E.T. (1972). Triglycine sulphate/selenate solid solutions for pyroelectric applications. *Ferroelectrics*, **4**, 253.

Cerevenka, P.O., Prasad Rao, A.O. and Porto, S.P.S. (1976). The ferroelectric phase transition and dielectric anomaly in tri-glycine sulphate. *Ferroelectrics*, **11**, 511.

Chandan, N.K. and Bajpai, P.K. (2002). Unpublished result.

Gaffar, M.A. and Abu El-Fadl, A. (1988). Physical properties of triglycine sulphate crystals containing different concentrations of Ni2+. *Ind. J. Pure & Appl. Phys*., **26**, 28.

Hoshino, S., Okaya, Y. and Pepinsky, R. (1959). Crystal structure of the ferroelectric phase of $(Glycine)_3.H_2SO_4$. *Phys. Rev*., **115**, 323.

Huong, P.V. and Hilczer, B. (1981). Behaviour of hydrogen bounded ferroelectrics KH_2PO_4 and KD_2PO_4 at high temperature. *J. Chem. Phys.*, **72**, 4412.

Jin, M. and Bhalla, A.S. (1995). Study of distribution of organic dopants in TGS crystal using micro-probe Raman spectroscopy. *Ferroelectrics*, **173**, 105.

Kampysheva, L.N., Golitsyna, O.M., Drozhdin, S.N., Moslikov, A.D. and Barbashina, A.V. (1995). Investigation of pulse polarization switching of irradiated triglycine sulphate crystals. *Physics of Solid State*, **37**, 209.

Komyak, A.I., Malyarevich, A.M. and Posledovich, M.R. (1993). Raman spectroscopy study of hydrogen bonds and vibration of the tri-glycine sulphate crystal lattice. *J. Appl. Spectroscopy*, **59**, 832.

Koneko, N., Takihashi, H. and Higasi, K. (1974). Temperature dependence of lattice vibrations of tri-glycine sulphate. *Bull. Chem. Soc. Japan*, **47**, 1148.

Lock, P.J. (1971). Effect of alanine substitution on TGS crystals. *Phys. Lett.* (*USA*), **19**, 390.

Malyarevich, A.M. and Posledovich, M.R. (1996). Phase transition and vibrational spectra of crystals of tri-glycine sulphate family. *J. Appl. Spectroscopy*, **63**, 865.

Matthias, B.T., Miller, C. and Remeika, J.P. (1956). Crystal structure of triglycine sulphate. *Phys. Rev.*, **104**, 849.

Quilichini, M., Krauzman, M. and Poulet, H.C.R. (1969). Raman scattering from ferroelectric crystals. *Acad. Sci. Paris Section. B.*, **269**, 774.

Ravi, G., Arunmozhi, G., Aravazhi, S., Anubukumar, S. and Ramasamy, S. (1994). *Proceedings of 4th International Conference on Properties and Applications of Dielectric Materials*, **1**, 247.

Santra, L., Verma, A.L., Bajpai, P.K., Hilczer, B. and Houng, P.V. (1994). Raman spectroscopic study of alanine doped tri-glycine sulphate ferroelectric single crystals. *J. Phys. Chem. Solids*, **55**, 405.

Schaack, G. and Winterfeldt, V. (1977). Temperature behaviour of optical phonons near Tc in triglycine sulphate and tri-glycine selenate-II. Evidence of non-linear pseudo-spin-phonon interaction. *Ferroelectrics*, **15**, 135.

Stankowska, J., Czernecka, A., Mielcarek, S. and Stabolepsza, K. (1994). Dielectric properties of tri-glycine sulphate crystals admixtured with L-threonine. *Ferroelectrics*, **158**, 163.

Winterfeldt, V., Schaack, G. and Klopperpieper, A. (1977). Temperature behaviour of optical phonons near T_c in triglycine sulphate and tri-glycine selenate-I. Infra-red reflection and Raman spectra. *Ferroelectrics*, **15**, 21.